Porphyrin-Cored Star Polymers as Efficient Nondoped Red Light-Emitting Materials

Binsong Li,[†] Xinjun Xu,[‡] Minghao Sun,[†] Yaqin Fu,[†] Gui Yu,[‡] Yunqi Liu,*[,‡] and Zhishan Bo*[,†]

State Key Laboratory of Polymer Physics and Chemistry, CAS Key Lab of Organic Solids, Institute of Chemistry, Chinese Academy of Sciences, Beijing 100080, China

Received July 22, 2005

Revised Manuscript Received November 1, 2005

Introduction

Organic and polymeric light-emitting diodes (OLEDs and PLEDs) have attracted tremendous interest in the large-area flat-panel displays due to their high brightness, low operation voltage, fast response, and cost-effective solution processability.[1] For the full-color displays, three primary colors, i.e., blue, green, and red, are required. Only the green light-emitting materials fully meet the requirements for the commercial applications.[2] For the blue light-emitting materials, high brightness and efficiency have been achieved, and the main problems are their stabilities and lifetimes. Red light-emitting is usually achieved by doping the red dyes such as porphyrins,[3] pyran-containing compounds,[4] and europium chelate complexes[5] into the wide-band-gap host materials. However, the optimum dopant concentration is usually very low and the effective doping range is very narrow.[4a] The doped red dyes are prone to aggregation in solid film at higher doping concentration, which usually leads to self-quenching of their fluorescence and results in lower efficiency for the devices. At lower doping concentration, the energy transfer from the host materials to the guest (red dyes) is often incomplete, which brings about poor color purity for the devices.[4b,6] Furthermore, for the practical application, LEDs based on dopant are more difficult to adapt for mass production processes than those based on a nondoped host emitter.[7]

In our previous paper, a set of well-defined and monodisperse porphyrin-cored star-shaped oligomers, as a kind of nondoped red-emissive molecular materials, were prepared, and their absorption and photoluminescence properties were investigated.[8] These monodisperse oligomers exhibited good solubility in common organic solvents and high quantum yields. However, the preparation of the monodisperse, well-defined star-shaped oligomers was usually time-consuming, and the column chromatography purification was usually required in each step. The difficulty of preparation limited them to be used as materials. For practical application, a low-cost large-scale synthesis is urgently required. Here, we report a simple one-pot approach to prepare porphyrin-cored star polymers and the investigation of their photo- and electroluminescent properties. Furthermore, to improve the hole transfer ability and the thermal stability of the porphyrin-cored star polymers, triphenylamine (TPA) was introduced as the end groups.[9] The cyclic voltammetry measurements indicated that the TPA-capped star porphyrin had higher HOMO energy level than the fluorene-capped star porphyrin did. The introduction of TPA end groups also reduced the energy barrier for the hole injection from ITO to the star porphyrin layer.

Experimental Section

Materials. All chemicals were purchased from Aldrich or Acros and used without further purification. 2-Bromo-7-trimethylsilyl-9,9-dioctylfluorene (**1**),[8] 2-bromo-9,9-dioctylfluorenyl-4,4,5,5-tetramethyl-[1,3,2]-dioxaborane (**4**),[10] fluorene-2-boronic acid (**5**),[8] triphenylamine monoboronic pinacol ester (**6**),[11] tetrakis(2-bromo-9,9-dioctylfluorenyl)porphyrin (**F1(Br)P**),[8] and monodisperse porphyrin-cored star-shaped oligomers (**FnP**, $n = 1-4$)[8] were synthesized according to the literature procedures. The catalyst precursor $Pd(PPh_3)_4$ was prepared according to the literature[12] and stored in a Schlenk tube under nitrogen.

Characterization. The gel permeation chromatography (GPC) measurements were performed on a Waters chromatograph connected to a Waters 410 refractive index detector with polystyrenes or monodisperse porphyrin oligomers as reference standards and tetrahydrofuran (THF) as an eluent. Three Waters Styragel column (HT2, 3, 4) connected in series were used. The ^{1}H and ^{13}C NMR spectra were recorded on a Bruker DM300 spectrometer in $CDCl_3$ at room temperature. The matrix-assisted laser desorption ionization time-of-flight (MALDI-TOF) mass spectroscopy measurements were carried out with a Bruker BIFLEXIII mass spectrometer with α-cyano-4-hydroxycinnamic acid (CCA) as the matrix. Elemental analyses were performed on a Flash EA 1112 analyzer or Carlo Erba 1106 analyzer. Thermal gravimetric analysis (TGA, Perkin-Elmer Pyris 1) and the differential scanning calorimetry (DSC, Mettler Toledo, DSC822e) measurements were carried out under a nitrogen atmosphere at a heating rate of 10 °C/min. UV−vis absorption spectra were recorded on a Shimadzu spectrometer model UV-1601 PC. Emission spectra were measured at room temperature with a Hitachi F-4500 fluorescence spectrophotometer. Fluorescence quantum yields (Φ_F) of the samples in toluene were determined by using tetraphenylporphyrin (TPP) ($\Phi_F = 0.11$ in toluene)[13] as a standard. Current−voltage characteristics were measured with a Hewlett-Packard 4140B semiconductor parameter analyzer. The luminescence output was measured by a Newport 2835-C multifunction optical meter. Cyclic voltammetry (CV) measurements were performed on a CHI630a electrochemical analyzer.

7-Trimethylsilyl-9,9-dioctylfluorene-2-aldehyde (2). To a stirred solution of **1** (8.34 g, 15.40 mmol) in absolute ether (50 mL) was added dropwise a solution of *n*-BuLi (5.90 mL, 2.89 M in hexane, 17.05 mmol) at −78 °C under nitrogen. The mixture was stirred at this temperature for 0.5 h and then allowed to warm to room temperature; thereafter, it was cooled to −78 °C again. DMF (3.60 mL) was added; the mixture stirred overnight and allowed to warm to room temperature gradually. Then 50 mL HCl (2 M) was added, and the mixture was stirred for 2 h. The organic layer was separated, the aqueous layer extracted twice with 100 mL of ether, and the combined organic layer dried over Na_2SO_4. After removal of the solvent, the crude product was purified by column chromatography (silica gel, hexane to hexane/CH_2Cl_2 = 3:1 v/v) to afford a colorless solid (6.80 g, 90%). ^{1}H NMR (300 MHz, $CDCl_3$): δ (ppm) 10.05 (s, 1H), 7.86 (d, 3H), 7.75 (d, 1H), 7.54 (s, 1H), 7.51 (d, 1H), 2.03−1.97 (broad, 4H), 1.20−1.03 (broad, 20H), 0.82−0.78 (broad, 6H), 0.59 (broad, 4H), 0.32 (s, 9H). ^{13}C NMR (75 MHz, $CDCl_3$): δ (ppm) 192.4, 151.7, 151.2, 147.5, 141.5, 140.0, 135.3, 132.0, 130.5, 127.7, 123.1, 120.1, 120.0, 55.1, 39.9, 31.7, 29.9, 29.8, 29.1, 23.7, 22.6, 14.0, −1.0. Anal. Calcd for $C_{33}H_{50}OSi$: C, 80.75; H, 10.27. Found: C, 79.91; H, 9.40.

7-Iodo-9,9-dioctylfluorene-2-aldehyde (3). A solution of ICl (17.10 mL, 1.0 M in CH_2Cl_2, 17.10 mmol) was added dropwise to a solution of **2** (7.0 g, 14.26 mmol) in CH_2Cl_2 (200 mL) at 0 °C. The solution was stirred overnight at room temperature under darkness, 0.1 M aqueous NaOH was added until the red color turned to colorless, the organic layer separated, the aqueous layer extracted

[†] State Key Laboratory of Polymer Physics and Chemistry.
[‡] CAS Key Lab of Organic solids.
* To whom correspondence should be addressed. E-mail: zsbo@iccas.ac.cn.

10.1021/ma051610s CCC: $33.50
Published on Web 12/01/2005

Chart 1

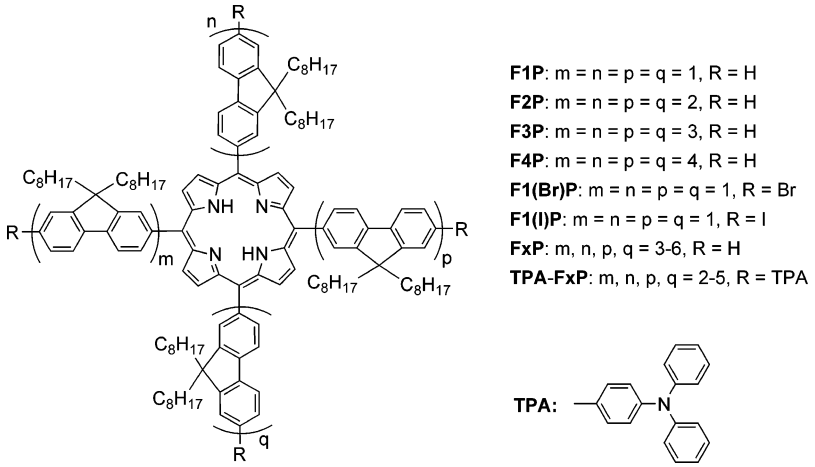

with CH_2Cl_2 (2 × 100 mL), and the combined organic layer dried over Na_2SO_4 and evaporated to dryness. The residue was purified by column chromatography (silica gel, hexane/CH_2Cl_2) to give **3** as a white solid (7.43 g, 96%). ^{1}H NMR (300 MHz, $CDCl_3$): δ (ppm) 10.05 (s, 1H), 7.86 (d, 2H), 7.81 (d, 1H), 7.71 (d, 2H), 7.52 (d, 1H), 2.05−1.90 (broad, 4H), 1.22−1.03 (broad, 20H), 0.83−0.80 (broad, 6H), 0.55 (broad, 4H). ^{13}C NMR (75 MHz, $CDCl_3$): δ (ppm) 191.77, 153.86, 150.43, 145.95, 138.66, 135.80, 135.24, 131.88, 130.07, 122.57, 122.02, 119.66, 94.44, 55.04, 39.55, 31.24, 29.33, 28.80, 28.66, 23.19, 22.10, 13.59. Anal. Calcd for $C_{30}H_{41}IO$: C, 66.17; H, 7.59. Found: C, 66.16; H, 7.48.

Tetrakis(2-iodo-9,9-dioctyl-fluorenyl)porphyrin (F1(I)P). A mixture of 7-iodo-9,9-dioctylfluorene-2-aldehyde, **3** (0.19 g, 10 mM), pyrrole (24 μL, 10 mM), and $CHCl_3$ was purged with nitrogen for 10 min before trifluoroacetic acid (40 μL, 0.52 mmol, 15 mM) was added and stirred at room temperature overnight. DDQ (86 mg, 11 mM) was added, and the mixture was stirred for a further 5 h before triethylamine (72 μL, 0.52 mmol, 15 mM) was added. The entire reaction mixture was filtered through a short column ($CHCl_3$ as an eluent) to afford the crude porphyrins. Further chromatography (silica gel, CH_2Cl_2/hexane = 1:3 v/v) gave the product as purple solids (98 mg, 48%). ^{1}H NMR (300 MHz, $CDCl_3$): δ (ppm) 8.90 (d, 8H), 8.21 (d, 8H), 8.04 (d, 4H), 7.81 (d, 8H), 7.70 (d, 4H), 2.09 (broad, 16H), 1.14 (broad, 80H), 0.98−0.88 (broad, 16H), 0.73 (broad, 24H), −2.63 (s, 2H). Anal. Calcd for $C_{136}H_{170}I_4N_4$: C, 68.97; H, 7.23; N, 2.37. Found: C, 69.09; H, 7.21; N, 2.59.

General Procedure for the Synthesis of Porphyrin-Cored Star Polymers. Porphyrin-cored star polymers **FxP** and **TPA-FxP** were prepared through the palladium-catalyzed Suzuki polycondensation of **F1(I)P** (0.18 g, 76.0 μmol) and AB-type monomer (**4**) (0.46 g, 765.6 μmol) in a biphasic mixture ($NaHCO_3$ (1.60 g, 19.0 mmol), THF (40 mL), toluene (40 mL), and H_2O (40 mL)) with $Pd(PPh_3)_4$ (6.0 mg, 5.2 μmol) as the catalyst precursor. The bromo end groups were blocked with 9,9-dioctylfluorenyl-2-boronic acid (**5**) (0.20 g, 456.0 μmol) or triphenylamine monoboronic pinacol ester (**6**) (0.17 g, 456.0 μmol). The organic layer was separated, washed with the saturated NaCl solution, and then evaporated to dryness. The crude products were purified by flash chromatography on acidic silica gel eluting with CH_2Cl_2/hexane increasing to THF to give **FxP** free of linear oligomers. (In the case of **TPA-FxP**, after column separation, precipitation from THF into ethanol/hexane (4:1, v/v) afforded the desired TPA-capped star polymers.) Thin-layer chromatography (TLC) and MALDI-TOF mass spectroscopy were used to inspect the purity of porphyrin-cored star polymers.

FxP: Yield 64%. ^{1}H NMR (300 MHz, $CDCl_3$): δ 9.01−8.96 (broad, 8H), 8.60 (broad, 4H), 8.28 (broad, 8H), 8.14−8.04 (broad, 12H), 7.88−7.60 (broad, 108H), 7.37−7.34 (broad, 16H), 2.13−2.06 (broad, 80H), 1.14 (broad, 400H), 0.83−0.73 (broad, 200H), −2.53 (broad, 2H).

TPA-FxP: Yield 61%. ^{1}H NMR (300 MHz, $CDCl_3$): δ 9.01−8.96 (broad, 8H), 8.59 (broad, 4H), 8.27−8.25 (broad, 8H), 8.13−8.03 (broad, 12H), 7.86−7.58 (broad, 72H), 7.32−7.26 (broad, 24H), 7.20−7.15 (broad, 24H), 7.07−7.02 (broad, 8H), 2.40−2.32 (broad, 64H), 1.15 (broad, 320H), 0.81−0.74 (broad, 160H), −2.52 (broad, 2H).

Results and Discussion

Synthesis and Characterization. The structures of the porphyrin-cored monodisperse oligomers and polydisperse polymers are shown in Chart 1. Scheme 1 shows the synthetic routes to the porphyrin monomer and the porphyrin-cored star oligomers and polymers. Starting from 2-bromo-7-trimethylsilyl-9,9-dioctylfluorene (**1**), its treatment with 1.2-fold of *n*-BuLi, followed by quenching with dimethylformamide (DMF), gave 7-trimethylsilyl-9,9-dioctylfluorene-2-aldehyde (**2**) in a yield of 90%. The TMS group was readily converted to the iodo group by treatment with ICl in CH_2Cl_2. 7-Iodo-9,9-dioctylfluorene-2-aldehyde (**3**) was obtained in a yield of 96%. Condensation of **3** and pyrrole in chloroform with trifluoroacetic acid (TFA) as a catalyst afforded the key monomer, 5,10,15,20-tetrakis(2-iodo-9,9-dioctylfluorene-7-yl)porphyrin (**F1(I)P**), in a yield of 48%. The fluorene- and TPA-capped porphyrin-cored star polymers **FxP** and **TPA-FxP** were synthesized by a one-pot Suzuki polycondensation (SPC). The SPC of porphyrin core (**F1(I)P**) and AB-type monomer (**4**) was carried out in a biphasic mixture of THF/toluene/aqueous $NaHCO_3$ with $Pd(PPh_3)_4$ as a catalyst precursor. Since the reaction of arylboronic acid (or ester) proceeds at a higher rate with iodoaromatics than with bromoaromatics, the polymerization should proceed in a core **(F1(I)P)** first fashion. After the polymerization, the bromo end groups were completely blocked with fluorene-2-boronic acid (**5**) or triphenylamine monoboronic pinacol ester (**6**). Inevitably, a small amount of linear oligofluorenes could form and intermix into the desired polymers. Because of the polarity difference, the linear oligofluorenes could be easily removed from the desired fluorene-capped star polymers by flash chromatography on silica gel. For triphenylamine-capped star polymers, after flash chromatography, precipitation from THF into hexane/ethanol (1:4, v:v) was required to remove the linear oligomers. Thin-layer chromatography (TLC) and MALDI-TOF mass spectroscopy verified the isolation. The fluorene-capped star polymer **FxP** and the triphenylamine-capped star polymer **TPA-FxP** were obtained in moderate yields (64% and 61%). The chemical structures of the polymers were confirmed by ^{1}H NMR spectra, element analysis, and MALDI-TOF mass spectroscopy. The element analysis results showed that the bromine contents of **FxP** and **TPA-FxP** were both below the detection limit (0.3%), which indicated that all the bromo end groups were capped with fluorene or triphenylamine.

Scheme 1. Synthetic Routes to F1(I)P and Porphyrin-Cored Star Polymers FxP and TPA-FxP

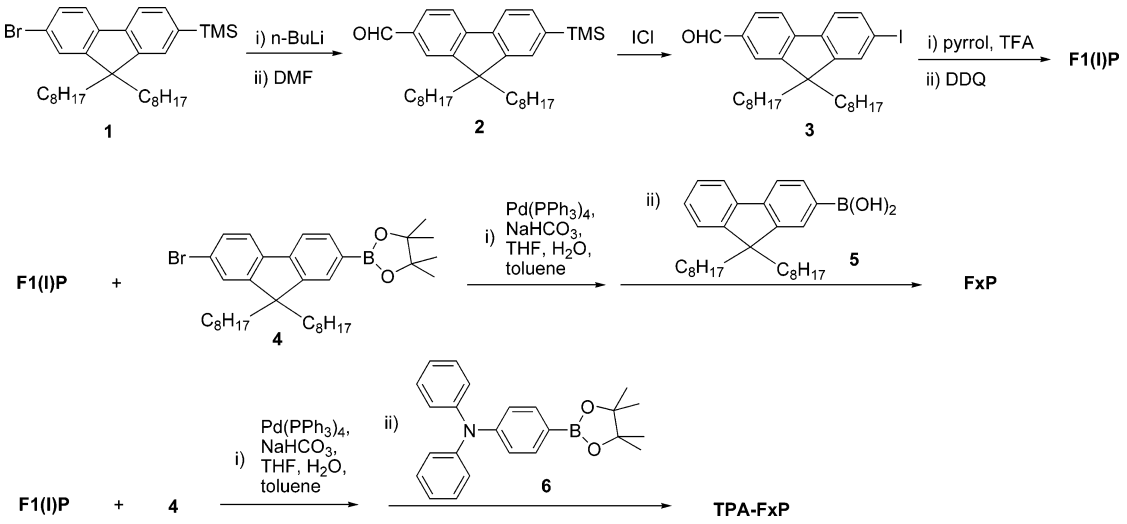

Table 1. Molecular Weights and Polydispersities (PD) of Porphyrin-Cored Polymers

	GPC (PS as standards)			GPC (FnP as standards)			MALDI-TOF MS	calcd
samples	M_n	M_w	PD	M_n	M_w	PD		
F1P	2400	2500	1.01				1863	1865
F2P	5000	5200	1.03				3416	3419
F3P	9800	9900	1.02				4975	4974
F4P	14800	15100	1.02				6533	6528
FxP	10200	20100	1.98	7000	9900	1.40	5379[a]	7306[b]
TPA-FxP	10200	21600	2.11	7100	10300	1.45	4405[a]	6724[b]

[a] The dominant molecular weight. [b] Calculated according to the feed ratios of the starting materials.

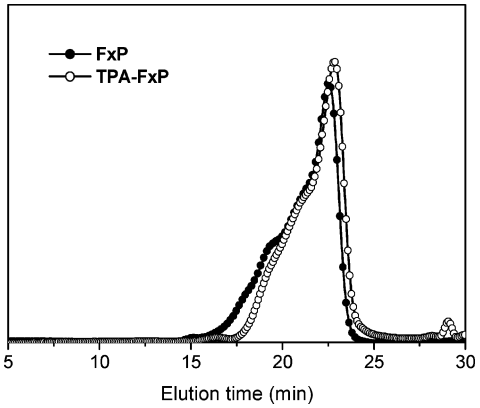

Figure 1. GPC elution curves of porphyrin-cored star polymers.

Porphyrin-cored star polymers **FxP** and **TPA-FxP** exhibited good solubility in common organic solvents such as dichloromethane, chloroform, THF, and toluene. The molecular weights and polydispersity of **FxP** and **TPA-FxP** were determined with gel permeation chromatography (GPC). The GPC elution traces are shown in Figure 1. Considering the large discrepancy of molecular weights obtained by GPC calibrated with polystyrene standards with the real molecular weights of the monodisperse oligomers, monodisperse star-shaped oligomers were also used as GPC standards to determine the molecular weight of the star polymers. The results are summarized in Table 1. The number-average molecular weights and polydispersities of both **FxP** and **TPA-FxP** were around 10 200 and 2.0, respectively, when using PS as standards. These values changed to 7000 and 1.4, respectively, when using **FnP** as the calibration standards. The molecular weights of **FxP** and **TPA-FxP** determined by MALDI-TOF mass spectroscopy were in the range of 4600−7300 and 4000−5200, respectively (see Supporting Information). It is obvious that the molecular weights determined by GPC calibrated with monodisperse oligomer standards are closer to the real molecular weights than those determined by GPC with PS standards.

Photoluminescent, Electroluminescent, Electrochemical, and Thermal Properties. The normalized solution and film absorption spectra of **FxP** and **TPA-FxP** are shown in Figure 2. In THF solution, all polymers exhibited a broad absorption band from 300 to 400 nm, an intensive Soret band at 430 nm, and four weak Q-bands in the range of 500−700 nm. The absorption in blue region was due to the oligofluorene arms, and the Soret and Q-bands absorption was due to the porphyrin core. Additionally, **TPA-FxP** also showed an absorption peak of TPA segments at about 310 nm. Compared with the solution absorption spectra, the Soret bands in film ones were only red-shifted for about 4 nm. In film, no significant peak broadening, which was normally due to the aggregation of the porphyrin rings, was found.[8]

The normalized photoluminescent (PL) spectra of **FxP** and **TPA-FxP** in THF solution and film are also shown in Figure 2. In solution, **FxP** and **TPA-FxP** exhibited emissions in both blue and red regions. The residual blue emission was due to the incomplete energy transfer from oligofluorene arms to the porphyrin core. The singlet−singlet energy transfer efficiency for **FxP** and **TPA-FxP** were ca. 94% and 92%, respectively, as estimated from the ratio of normalized corrected excitation spectrum and absorption spectrum at 430 nm (the absorption maximum of porphyrins).[14] The polymer films were obtained by spin-coating a 10 mg/mL solution in THF at 1800 rpm. In films, **FxP** and **TPA-FxP** displayed only an intensive red emission peak at around 663 nm with a shoulder at 726 nm, while the emissions from the oligofluorene segments disappeared. The more efficient energy transfer in film than in solution was probably due to the smaller torsion angle between porphyrin and fluorene[8] as well as the shorter chromophore distances and efficient intermolecular exciton mobility in film. In comparison, the doping of PFs film with TPP in different concentrations was also investigated. Compared with the star polymer film emission spectra, the TPP/PFs film had an emission band in the blue region and two blue-shifted peaks centered at 651 and 719 nm in the red region (Figure S6). The TPP/PFs film showed dominantly red emission only when the concentration of TPP was larger than 4 wt %. There still

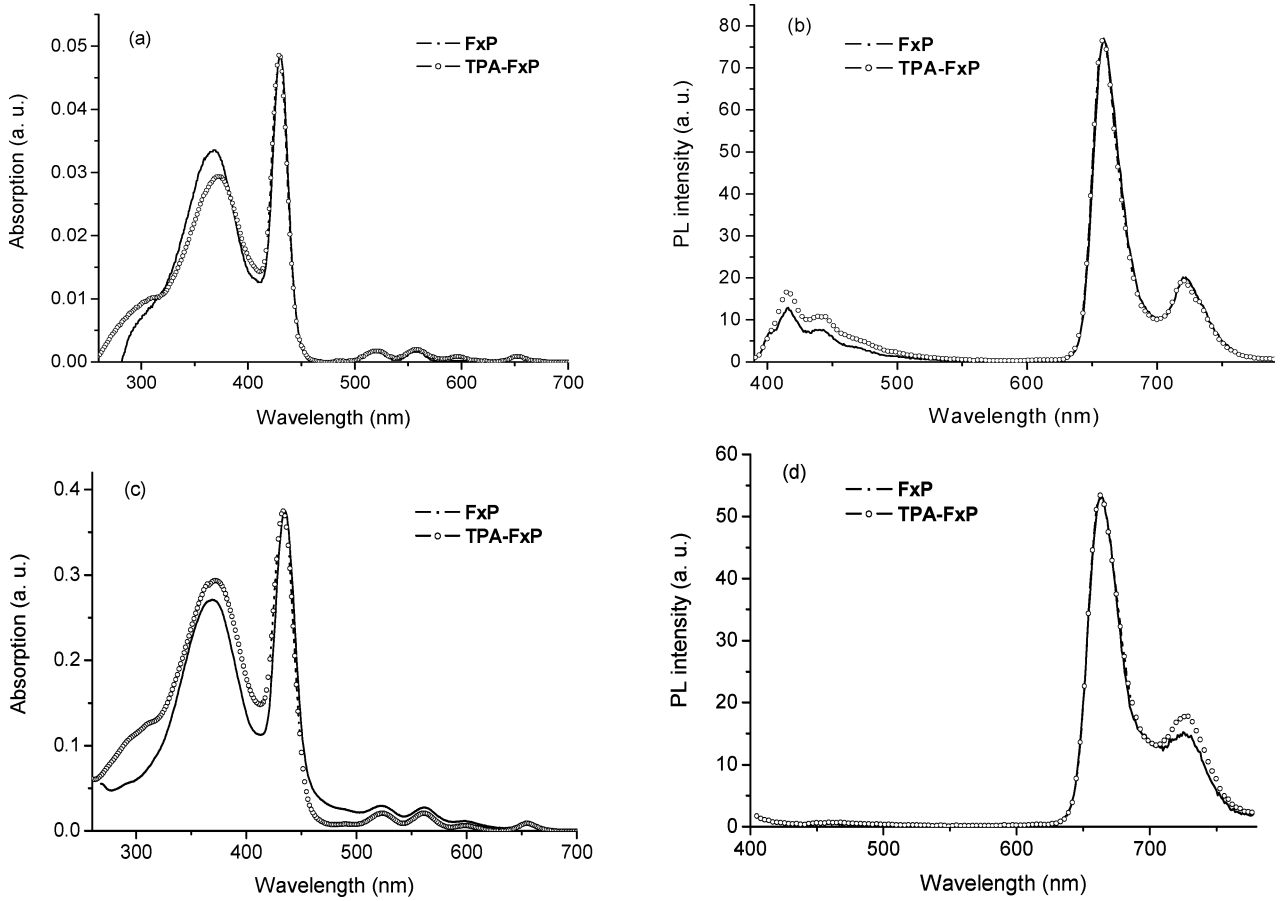

Figure 2. Normalized UV−vis absorption (a) and photoluminescence spectra (b) of **FxP** and **TPA-FxP** in THF (excited at 360 nm, the molar extinction coefficient was ca. 7×10^5 M^{-1} cm^{-1}). The normalized UV−vis absorption (c) and photoluminescence spectra (d) of **FxP** and **TPA-FxP** in films (excited at 395 nm).

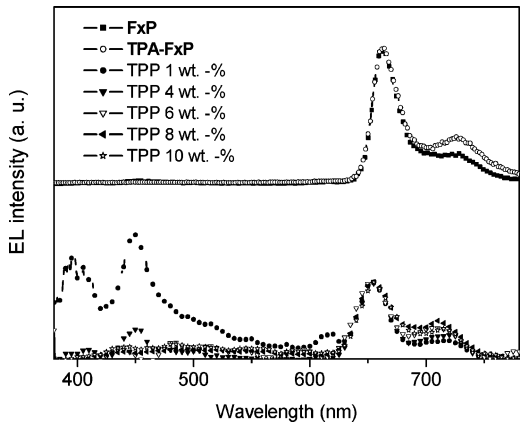

Figure 3. Electroluminescence spectra of PLEDs based on **FxP** and **TPA-FxP** and TPP/PFs.

remained a tiny peak at 437 nm even when the concentration of TPP was up to 8 wt %. It was probably due to the less efficient through-space (Förster) energy transfer from the PFs to the TPP. The fluorescence quantum yields (Φ_F) of **FxP** and **TPA-FxP** in dilute toluene solution with TPP ($\Phi_F = 0.11$) as the reference standard (irradiated at 423 nm) were 0.17 for both **FxP** and **TPA-FxP**.

A single-layer PLED device with the configuration of ITO/PEDOT:PSS/polymer/Al was fabricated. The electroluminescence spectra of PLEDs based on **FxP**, **TPA-FxP**, and TPP/PFs are shown in Figure 3. The PLEDs of **FxP** (or **TPA-FxP**) showed only a deep red emission at about 662 nm (663 nm for **TPA-FxP**) and a shoulder at 726 nm (727 nm for **TPA-FxP**). The complete disappearance of the blue emission from the oligofluorene segments indicated that an efficient energy transfer from oligofluorene segments to porphyrin cores occurred. The doped devices emitted pure red light only when the TPP concentration was higher than 6 wt %, while at this concentration the TPP had already intensively aggregated (the EL peak red-shifted and became broader when the concentration of TPP was larger than 6 wt %) and self-quenched of their fluorescence, leading to a dramatic decrease in their fluorescence quantum yields.[3a] The dilemma of incomplete energy transfer and concentration quenching in the doped PLEDs was readily resolved by the use of nondoped porphyrin-cored star polymers.

The electrochemical behaviors of porphyrin-cored star polymers were investigated by using cyclic voltammetry (CV) with a standard three-electrode electrochemical cell in acetonitrile solution containing 0.1 M tetrabutylammonium hexafluorophosphate ($TBAPF_6$) at room temperature. The oxidation potentials were measured vs $Ag/AgNO_3$ as a reference electrode and a standard ferrocene/ferrocenium redox system as the internal standard for estimating the HOMO of the polymer films. The polymer films on the work electrodes were deposited by casting from chloroform solution. The CV curves of polymer **FxP** and **TPA-FxP** in film are shown in Figure 4. In the range of 0 and 1.4 V, the **FxP** film displayed one oxidation peak at 1.23 V. For polymer **TPA-FxP**, the film showed four oxidation peak at 0.62, 0.66, 1.10, and 1.18 V. The first and second oxidation peaks were relatively weak (inset of Figure 4b). Taking −4.80 eV as the HOMO level for the ferrocene/ferrocenium redox system, HOMO levels of −5.71 and −5.20 eV were calculated for **FxP** and **TPA-FxP** films, respectively. The band gaps of

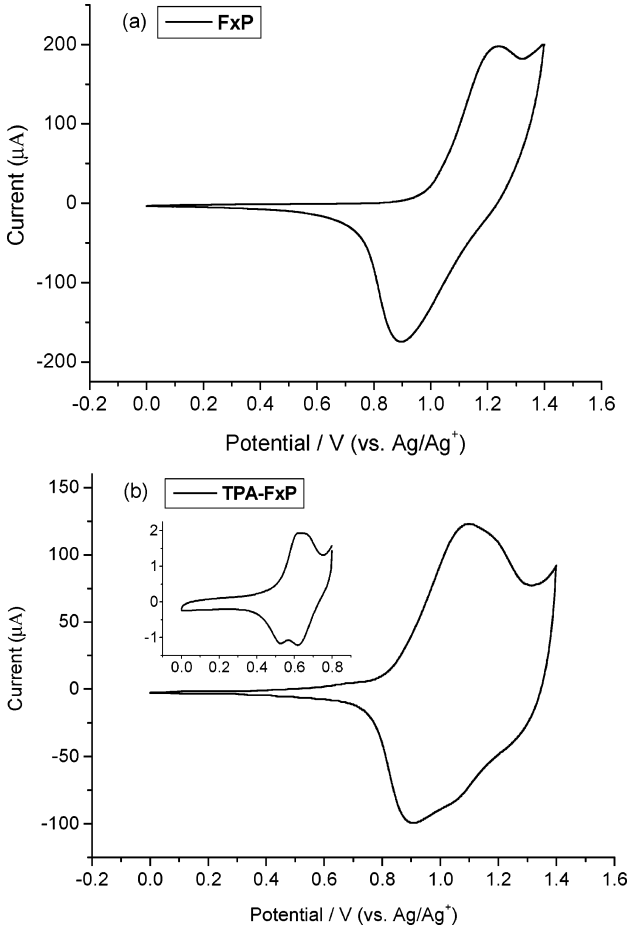

Figure 4. Cyclic voltammograms of the electrochemical oxidation of **FxP** (a) and **TPA-FxP** (b) in films at a sweep rate of 10 mV/s.

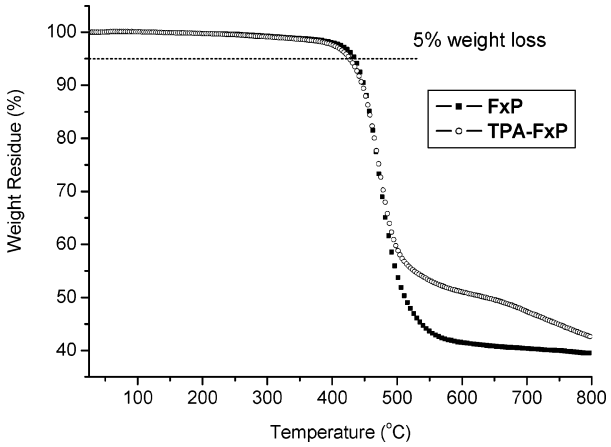

Figure 5. TGA traces of porphyrin-cored polymers.

FxP and **TPA-FxP** calculated from the UV−vis absorption onset of the films were both 1.83 eV. The LUMO levels of polymer **FxP** and **TPA-FxP** in film were estimated to be −3.88 and −3.37 eV, respectively. The HOMO energy levels of porphyrin-cored polymers were both higher than that of polyfluorene films (−5.8 eV),[15] which implied a much lower barrier for the hole injection in nondoped porphyrin-cored polymer devices than that in the TPP/PFO-doped systems. In comparison with the HOMO energy level of **FxP**, the HOMO energy levels of **TPA-FxP** increased markedly, which was due to the introduction of TPA end group.[9] The increasing of the HOMO energy levels endowed TPA-capped porphyrin-cored polymers with even better hole-transfer ability. The good hole-transfer ability of **TPA-FxP** was also proved by the lowest turn-on voltage of single-layer PLEDs (9 V for the **TPA-FxP** device, 10 V for the **FxP** device, and 30 V for the TPP/PFs blend device; the turn-on voltage was defined as the bias required to give a luminance of 1 cd/m^2).

The thermal properties of the porphyrin-cored polymers (**FxP** and **TPA-FxP**) and monodisperse oligomers (**FnP**) were investigated with thermogravimetric analyses (Figure 5 and Figure S7) and differential scanning calorimetry (Figure S8). All the polymers exhibited good thermal stability. They showed less than 5% weight loss at 430 °C. The thermal stability increased slightly with the increasing of the molecular weights (Figure S7). No clear glass transition was observed in the second heating scan of DSC curves of porphyrin-cored polymers.

Conclusions

In conclusion, we have developed an easy one-pot approach to prepare porphyrin-cored star polymers on the gram scales. Fluorene and triphenylamine were used to cap the bromo end groups. The polymer structures were well characterized. The porphyrin-cored star polymers exhibited good solubility and film-forming ability. The photoluminescence and electroluminescence of these porphyrin-cored polymers displayed pure saturated red light emission. The cyclic voltammetry results indicated that the HOMO energy levels of oligofluorene-arm star porphyrins were much higher than that of PFs. The devices based on the porphyrin-cored star polymers displayed much lower turn-on voltages than those of the devices based on TPP/PFs. The introduction of TPA end groups endowed the polymers with even higher HOMO energy level and even lower turn-on voltage of the devices.

Acknowledgment. Financial support from the National Natural Science Foundation of China (20225415, 20374053, 90206049, and 20472089) and the Major State Basic Research Development Program (2002CB613401 and 2001CB610507) is greatly acknowledged.

Supporting Information Available: ^{1}H NMR and MALDI-TOF spectra of porphyrin-cored polymers as well as additional fluorescence spectra and thermal characterization. This material is available free of charge via the Internet at http://pubs.acs.org.

References and Notes

(1) (a) Burroughes, J. H.; Bradley, D. D. C.; Brown, A. B.; Marks, R. N.; Mackay, K.; Friend, R. H.; Bum. P. L.; Holmes, A. B. *Nature (London)* **1990**, *347*, 539. (b) Gross, M.; Müller, D. C.; Nothofer, H.-G.; Scherf, U.; Neher, D.; Bräuchle, C.; Meerholz, K. *Nature (London)* **2000**, *405*, 661. (c) Müller, D. C.; Falcou, A.; Reckefuss, N.; Rojahn, M.; Wlederhirm, V.; Rudati, P.; Frohne, H.; Nuyken, O.; Becker, H.; Meerhotz, K. *Nature (London)* **2003**, *421*, 829. (d) Hou, Q.; Zhang, Y.; Li, F. Y.; Peng, J. B.; Cao, Y. *Organometallics* **2005**, *24*, 4509.

(2) Kraft, A.; Grimsdale, A. C.; Holmes, A. B. *Angew. Chem., Int. Ed.* **1998**, *37*, 402.

(3) (a) Virgili, T.; Lidzey, D. G.; Bradley, D. D. C. *Adv. Mater.* **2000**, *12*, 58. (b) Burrows, P. E.; Forrest, S. R.; Silbley, S. P.; Thompson, M. E. *Appl. Phys. Lett.* **1996**, *69*, 2959. (c) Baldo, M. A.; O'Brien, D. F.; You, Y.; Shoustikov, A.; Sibley, S.; Thompson, M. E.; Forrest, S. R. *Nature (London)* **1998**, *395*, 151. (d) Kwong, R. C.; Sibley, S.; Dubovoy, T.; Baldo, M.; Forrest, S. R.; Thompson, M. E. *Chem. Mater.* **1999**, *11*, 3709. (e) Guo, T.-F.; Chang, S.-C.; Yang, Y.; Kwong, R. C.; Thompson, W. E. *Org. Electrochem.* **2000**, *1*, 15.

(4) (a) Tang, C. W.; Van Slyke, S. A.; Chen, C. H. *J. Appl. Phys.* **1989**, *65*, 3610. (b) Bulovic, V.; Shoustikov, A.; Baldo, M. A.; Bose, E.; Kozlov, V. G.; Thompson, M. E.; Forrest, S. R. *Chem. Phys. Lett.* **1998**, *287*, 455.

(5) (a) Kido, J.; Nagai, K.; Okamato, Y.; Skotheim, T. *Chem. Lett.* **1991**, 1267. (b) Kido, J.; Hayase, H.; Hongawa, K.; Nagai, K. Okuyama, K. *Appl. Phys. Lett.* **1994**, *65*, 2124.
(6) (a) Hamada, Y.; Kanno, H.; Tsujioka, T.; Takahashi, H.; Usuki, T. *Appl. Phys. Lett.* **1999**, *75*, 1682. (b) Tao, X. T.; Miyata, S.; Sasabe, H.; Zhang, G. J.; Wada, T.; Jiang, M. H. *Appl. Phys. Lett.* **2001**, *78*, 279. (c) Picciolo, L. C.; Murata, H.; Kafafi, Z. H. *Appl. Phys. Lett.* **2001**, *78*, 2378.
(7) (a) Chen, C.-T. *Chem. Mater.* **2004**, *16*, 4389. (b) Wu, W.-C.; Yeh, H.-C.; Chan, L.-H.; Chen, C. T. *Adv. Mater*. **2002**, *14*, 1072.
(8) Li, B. S.; Li, J.; Fu, Y. Q.; Bo, Z. S. *J. Am. Chem. Soc.* **2004**, *126*, 3430.
(9) (a) Miteva, T.; Meisel, A.; Knoll, W.; Nothofer, H. G.; Scherf, U.; Müller, D. C.; Meerholz, K.; Yasuda, A.; Neher, D. *Adv. Mater.* **2001**, *13*, 565. (b) Ego, C.; Grimsdale, A. C.; Uckert, F.; Yu, G.; Srdanov, G.; Müllen, K. *Adv. Mater.* **2002**, *14*, 809. (c) Shu, C.-F.; Dodda, R.; Wu, F.-I.; Liu, M. S.; Jen, A. K.-Y. *Macromolecules* **2003**, *36*, 6698.
(10) Sandee, A. J.; Williams, C. K.; Evans, N. R.; Davies, J. E.; Boothby, C. E.; Köhler, A.; Friend, R. H.; Holmes, A. B. *J. Am. Chem. Soc.* **2004**, *126*, 7041.
(11) Wong, K.-T.; Chien, Y.-Y.; Liao, Y.-L.; Lin, C.-C.; Chou, M.-Y.; Leung, M.-K. *J. Org. Chem.* **2002**, *67*, 1041.
(12) Tolman, C. A.; Seidel, W. C.; Gerlach, D. H. *J. Am. Chem. Soc.* **1972**, *94*, 2669.
(13) Seybold, P.; Gouterman, M. *J. Mol. Spectrosc.* **1969**, *31*, 1.
(14) (a) Devadoss, C.; Bharathi, P.; Moore, J. S. *J. Am. Chem. Soc.* **1996**, *118*, 9635. (b) Stryer, L.; Haugland, R. P. *Proc. Natl. Acad. Sci. U.S.A.* **1967**, *58*, 719. (c) Haugland, R. P.; Yguerabide, J.; Stryer, L. *Proc. Natl. Acad. Sci. U.S.A.* **1969**, *63*, 23. (d) Jiang, D. L.; Aida, T. *J. Am. Chem. Soc.* **1998**, *120*, 10895.
(15) (a) Yang, J.; Jiang, C. Y.; Zhang, Y.; Yang, R.; Yang, W.; Hou, Q.; Cao, Y. *Macromolecules* **2004**, *37*, 1211. (b) Xia, C. J.; Advincula, R. C. *Macromolecules* **2001**, *34*, 5854.

MA051610S